

## Synthesis and Characterization of an Air-Stable Gallium Hydride, $[t\text{-Bu(H)Ga}(\mu\text{-NEt}_2)_2]_2$ , and Related Chloride Derivatives

Luke Grocholl, Scott A. Cullison, Jianjun Wang, Dale C. Swenson, and Edward G. Gillan\*

Department of Chemistry and the Optical Science and Technology Center, University of Iowa, Iowa City, Iowa 52242-1294

Received December 14, 2001

The synthesis of  $[t\text{-Bu(H)Ga}(\mu\text{-NEt}_2)_2]_2$  (**1**) was accomplished by the addition of 4 *t*-BuLi to  $[\text{Cl}_2\text{Ga}(\mu\text{-NEt}_2)]_2$ . Evidence suggests that two *tert*-butyl groups are lost as isobutylene and result in Ga–H bond formation. The gallium hydride **1** is remarkably stable toward ambient air, oxygen, photolysis, and moderate heating; however, in  $\text{CHCl}_3$  the hydride is replaced by chloride, producing  $[t\text{-Bu(Cl)Ga}(\mu\text{-NEt}_2)_2]_2$  (**2**). Compound **1** may also be synthesized by sequential *tert*-butyl additions to  $[\text{Cl}_2\text{Ga}(\mu\text{-NEt}_2)]_2$ . A singly substituted *tert*-butyl dimer,  $t\text{-Bu(Cl)Ga}(\mu\text{-NEt}_2)_2\text{GaCl}_2$  (**3**), was also isolated, and interconversions between **1**, **2**, and **3** are described. Compound **1** was tested for utility in the chemical vapor deposition of GaN and produced gallium-rich films at low temperatures (<250 °C) with limited nitrogen incorporation due to facile  $\text{Et}_2\text{NH}$  elimination.

### Introduction

Group 13 nitrides are central to a class of light-emitting semiconductors that are becoming increasingly exploited in device applications such as high-intensity blue lasers and full color displays.<sup>1</sup> The heavier nitrides, GaN ( $E_g = 3.4$  eV) and InN ( $E_g = 1.9$  eV), have useful band gaps in the near-UV and visible range. These semiconductors are most often synthesized as thin films by dual source chemical vapor deposition (CVD) processes.<sup>2</sup> Recent work has shown that molecular single-source precursors are chemically and structurally attractive alternatives for the low-temperature synthesis of GaN films, powders, and nanostructured solids. Inorganic and organometallic single-source gallium precursors with nitrogen ligands consisting of azides,<sup>3–7</sup> amides,<sup>8–11</sup>

and hydrazines<sup>5</sup> have been utilized for GaN film and powder synthesis. Many of these molecular conversions are performed below 500 °C, in contrast to conventional dual-source methods that often require temperatures in excess of 900 °C.

In the gallium amide molecular precursor arena, organometallic diethylamido ( $-\text{NEt}_2$ ) derivatives are much less studied than their methyl counterparts, likely due to the frequently intractable nature of diethylamido products. An early report describes dimeric  $[n\text{-Bu}_2\text{Ga}(\mu\text{-NEt}_2)]_2$  produced from *n*-Bu<sub>3</sub>Ga and  $\text{Et}_2\text{NH}$ ,<sup>12</sup> and a gallium dihydride,  $[\text{H}_2\text{-Ga}(\mu\text{-NEt}_2)]_2$ , has been structurally characterized.<sup>13</sup> There are a significant number of other structurally characterized alkyl

\* Author to whom correspondence should be addressed. E-mail: edward-gillan@uiowa.edu.

- (1) (a) Matsuoka, T. *Adv. Mater.* **1996**, *8*, 469. (b) Morkoc, H.; Mohammad, S. N. *Science* **1995**, *267*, 51.
- (2) (a) Nakamura, S.; Mukai, T.; Senoh, M.; Nagahama, S.; Iwasa, N. *J. Appl. Phys.* **1993**, *74*, 3911. (b) Niebuhr, R.; Bachem, K.; Dombrowski, K.; Maier, M.; Pletschen, W.; Kaufmann, U. *J. Electron. Mater.* **1995**, *24*, 1531.
- (3) McMurrin, J.; Dai, D.; Balasubramanian, K.; Steffek, C.; Kouvetakis, J.; Hubbard, J. *Inorg. Chem.* **1998**, *37*, 6638.
- (4) Kouvetakis, J.; McMurrin, J.; Matsunaga, P.; O'Keefe, M.; Hubbard, J. L. *Inorg. Chem.* **1997**, *36*, 1792.
- (5) Lakhota, V.; Neumayer, D. A.; Cowley, A. H.; Jones, R. A.; Ekerdt, J. G. *Chem. Mater.* **1995**, *7*, 546.
- (6) (a) Devi, A.; Sussek, H.; Pritzkow, H.; Winter, M.; Fischer, R. A. *Eur. J. Inorg. Chem.* **1999**, 2127. (b) Devi, A.; Rogge, W.; Wohlfart, A.; Hipler, F.; Becker, H.; Fischer, R. A. *Chem. Vap. Deposition* **2000**, *6*, 245.

- (7) (a) Frank, A.; Stowasser, F.; Sussek, H.; Pritzkow, H.; Miskys, C. R.; Ambacher, O.; Giersig, M.; Fischer, R. *J. Am. Chem. Soc.* **1998**, *120*, 3512. (b) Manz, A.; Birkner, A.; Kolbe, M.; Fisher, R. *Adv. Mater.* **2000**, *12*, 569.
- (8) Hoffman, D. M.; Rangarajan, S. P.; Athavale, S. D.; Economou, D. J.; Liu, J.-R.; Zheng, Z.; Chu, W.-K. *J. Vac. Sci. Technol. A* **1996**, *14* (2), 306.
- (9) Park, H. S.; Waezsada, S. D.; Cowley, A. H.; Roesky, H. W. *Chem. Mater.* **1998**, *10*, 2251.
- (10) (a) Janik, J. F.; Wells, R. L. *Chem. Mater.* **1996**, *8*, 2708. (b) Janik, J. F.; Wells, R. L.; Coffey, J. L.; St. John, J. V.; Pennington, W. T.; Schimek, G. L. *Chem. Mater.* **1998**, *10*, 1613. (c) Micic, O. I.; Ahrenkiel, S. P.; Bertram, D.; Nozik, A. *J. Appl. Phys. Lett.* **1999**, *75*, 478.
- (11) (a) Hwang, J.-W.; Campbell, J. P.; Kozubowski, Hanson, S. A.; Evans, J. F.; Gladfelter, W. L. *Chem. Mater.* **1995**, *7*, 517. (b) Jegier, J.; McKernan, S.; Purdy, A. P.; Gladfelter, W. L. *Chem. Mater.* **2000**, *12*, 1003.
- (12) Haran, R.; Jouany, C.; Laurent, J.-P. *Bull. Soc. Chim. Fr.* **1968**, *1*, 458.
- (13) Lorberth, J.; Dorn, R.; Massa, W.; Wocadlo, S. *Z. Naturforsch.* **1993**, *48B*, 224.

gallium monohydrides and dihydrides that are most often formed using  $\text{LiGaH}_4$  or  $\text{GaH}_3$ .<sup>14–19</sup> In the work below we report the unexpected synthesis of a sterically bulky, dimeric diethylamido-bridged gallium hydride,  $[\textit{t}\text{-Bu}(\text{H})\text{Ga}(\mu\text{-NEt}_2)]_2$ , that is apparently formed via the  $\beta$ -hydride elimination of a *tert*-butyl substituent. This molecular solid is exceptionally *air-stable*; however, it decomposes at elevated temperatures. The synthesis and characterization of  $[\textit{t}\text{-Bu}(\text{H})\text{Ga}(\mu\text{-NEt}_2)]_2$  and related chloride derivatives are presented along with preliminary chemical vapor deposition (CVD) studies using  $[\textit{t}\text{-Bu}(\text{H})\text{Ga}(\mu\text{-NEt}_2)]_2$ .

## Experimental Section

**General Procedures.** The following reagents were used as received:  $\text{GaCl}_3$  (Aldrich, 99.99% anhydrous),  $\text{LiNEt}_2$  (Aldrich or Strem 95+%), *t*-BuLi (Aldrich, 1.7 M in pentane), ammonia (Air Products, anhydrous). All solvents were distilled from sodium/benzophenone and degassed prior to use. Schlenk techniques were used for all solution manipulations, and solids were handled under argon in a Vacuum Atmospheres MO-40M glovebox. Other starting materials,  $[\text{Cl}_2\text{Ga}(\mu\text{-NEt}_2)]_2$ <sup>20</sup> and  $[\textit{t}\text{-Bu}_2\text{Ga}(\mu\text{-Cl})]_2$ <sup>21</sup> were synthesized in a manner similar to previously published procedures. Solution NMR spectra were obtained with a Bruker AC 300 or WM 360 spectrometer. Electron impact mass spectrometry (EI MS) was performed on solid samples using a VG TRIO-1 quadrupole system. FTIR absorption characteristics were determined with a Nicolet Nexus 670 spectrometer using KBr pellets or films on Si wafers. Melting points (uncorrected) were determined with a Melt-Temp apparatus. Sonication and UV photolysis tests were performed with a Branson 2210 sonication bath and a Pyrex-jacketed Ace-Hanovia photochemical mercury lamp, respectively. Elemental analyses (C, H, N, Cl) were performed by Midwest Micro-labs (www.midwestlab.com) and Desert Analytics (www.desertanalytics.com). UV–vis spectra were obtained with an HP 8453 diode array spectrometer. Auger and X-ray photoelectron spectroscopy were performed on films on Si using a Perkin-Elmer scanning Auger system at 3 keV and PHI 5400 XPS system with Al K $\alpha$  excitation, respectively. Scanning electron images were obtained with a Hitachi S4000 field emission electron microscope. The methylene substituents on diethylamido groups consisted of overlapping doublets of quartets (dq) that were deconvoluted using NMR simulations.<sup>22</sup> The chemical shift data for methylene resonances reported in the sections below were resolved by comparison with simulated spectra (see Supporting Information, Figures S1–S3).

- (14) (a) Storr, A. *J. Chem. Soc. A* **1968**, 2605. (b) Storr, A.; Penland, A. D. *J. Chem. Soc. A* **1971**, 1237.  
 (15) (a) Luo, B.; Gladfelter, W. L. *Chem. Commun.* **2000**, 825. (b) Luo, B.; Young, V. G., Jr.; Gladfelter, W. L. *Inorg. Chem.* **2000**, 39, 1705.  
 (16) Luo, B.; Pink, M.; Gladfelter, W. L. *Inorg. Chem.* **2001**, 40, 307.  
 (17) (a) Cowley, A. H.; Gabbai, F. P.; Atwood, D. A.; Carrano, C. J.; Mokry, L. M.; Bond, M. R. *J. Am. Chem. Soc.* **1994**, 116, 1559. (b) Cowley, A. H.; Gabbai, F. P.; Isom, H. S.; Carrano, C. J.; Bond, M. R. *Angew. Chem., Int. Ed. Engl.* **1994**, 33, 1253. (c) Isom, H. S.; Cowley, A. H.; Decken, A.; Sissingh, F.; Corbelin, S.; Lagow, R. J. *Organometallics* **1995**, 14, 2400.  
 (18) Miinea, L.; Hoffman, D. M. *Polyhedron* **2001**, 20, 2425.  
 (19) Uhl, W.; Cuypers, L.; Graupner, R.; Molter, J.; Vester, A.; Neumuller, B. *Z. Anorg. Allg. Chem.* **2001**, 627, 607.  
 (20) Herberich, G. E.; Englert, U.; Posselt, D. *J. Organomet. Chem.* **1993**, 461, 21.  
 (21) (a) Kovar, R. A.; Derr, H.; Brandau, D.; Callaway, J. *Inorg. Chem.* **1975**, 14, 2809. (b) Atwood, D. A.; Cowley, A. H.; Jones, R. A.; Mardones, M. A.; Atwood, J. L.; Bott, S. G. *J. Coord. Chem.* **1992**, 25, 233.  
 (22) NUTS-NMR Utility Transform Software, 2D version, 1999, Acorn software.

**Synthesis of  $[\textit{t}\text{-Bu}(\text{H})\text{Ga}(\mu\text{-NEt}_2)]_2$  (1).** One-pot in situ (method 1) and stepwise (method 2) routes involving lithium chloride salt elimination were both utilized in the synthesis of **1**. In method 1, a Schlenk flask containing a slurry of  $\text{LiNEt}_2$  (1.5 g, 18.9 mmol) in 100 mL of toluene was cooled to  $-78^\circ\text{C}$ . A solution of  $\text{GaCl}_3$  (3.2 g, 18.2 mmol) dissolved in 30 mL of pentane was slowly added to the  $\text{LiNEt}_2$  slurry over a 30-min period. The reaction mixture was warmed to room temperature and stirred overnight. The resulting orange solution was recooled to  $-78^\circ\text{C}$ , and 1.7 M *t*-BuLi in pentane (23 mL, 39.1 mmol) was slowly added over a 30-min period. The reaction mixture was warmed to room temperature and stirred overnight. Soluble products were isolated by filtration, and a crude yellow product was purified by recrystallization in pentane.

In method 2,  $[\text{Cl}_2\text{Ga}(\mu\text{-NEt}_2)]_2$  was isolated from the first addition step and purified by recrystallization in pentane. Its physical properties were in agreement with those reported in the literature.<sup>20</sup> A Schlenk flask was charged with  $[\text{Cl}_2\text{Ga}(\mu\text{-NEt}_2)]_2$  (2.5 g, 5.8 mmol) dissolved in 50 mL of pentane. This solution was cooled to  $-78^\circ\text{C}$ , and a slight excess of 1.7 M *t*-BuLi in pentane (11.0 mL, 24.2 mmol) was slowly added over a 30-min period. The solution was filtered, and the solvent was concentrated and placed in a  $-20^\circ\text{C}$  freezer, where colorless plates of  $[\textit{t}\text{-Bu}(\text{H})\text{Ga}(\mu\text{-NEt}_2)]_2$  grew. Yield: 45–55% with either method. Mp:  $159^\circ\text{C}$  (dec).  $^1\text{H}$  NMR ( $\text{C}_6\text{D}_6$ ):  $\delta$  0.87 (t, 6H,  $\text{NCH}_2\text{CH}_3$ , 6.9 Hz), 1.24 (s, 9H,  $\text{C}(\text{CH}_3)_3$ ), 2.98 (dq, 2H,  $\text{NCH}_2\text{CH}_3$ ,  $^2J_{\text{HH}} = 13.1$  Hz,  $^3J_{\text{HH}} = 6.7$  Hz), 3.07 (dq, 2H,  $\text{NCH}_2\text{CH}_3$ ,  $^2J_{\text{HH}} = 13.1$  Hz,  $^3J_{\text{HH}} = 7.2$  Hz), 4.73 (s broad, GaH).  $^{13}\text{C}$  NMR ( $\text{C}_6\text{D}_6$ ):  $\delta$  12.2 ( $\text{NCH}_2\text{CH}_3$ ), 22.4 ( $\text{C}(\text{CH}_3)_3$ ), 31.2 ( $\text{C}(\text{CH}_3)_3$ ), 44.2 ( $\text{NCH}_2\text{CH}_3$ ). EI MS ( $m/z$ ,  $\text{M}^+ = [\textit{t}\text{-Bu}(\text{H})\text{Ga}(\text{NEt}_2)]_2$ ): 399 ( $\text{M}^+ - \text{H}$ ), 343 ( $\text{M}^+ - \textit{t}\text{-Bu}$ ), 285 ( $\text{M}^+ - 2 \textit{t}\text{-Bu} - \text{H}$ ), 269 ( $\textit{t}\text{-BuGa}_2\text{NEt}_2^+$ ), 213 ( $\text{Ga}(\text{NEt}_2)_2^+$ ), 198 ( $\textit{t}\text{-BuGaNEt}_2^+$ ), 142 ( $\text{GaNEt}_2^+$ ), 126 ( $\textit{t}\text{-BuGa}^+$ ). IR spectrum ( $\text{cm}^{-1}$ , KBr pellet): 2966, 2935, 2868, 2843, 1834, 1801, 1767, 1460, 1378, 1260, 1147, 1107, 1040, 794, 671, 600, 568, 548. Elemental analysis found (calcd based on  $\text{C}_{16}\text{H}_{40}\text{Ga}_2\text{N}_2$ ): C 47.03 (48.05), N 7.34 (7.00), H 9.85 (10.08). No residual chlorine was detected by bulk elemental analysis.

**Synthesis of  $[\textit{t}\text{-Bu}(\text{Cl})\text{Ga}(\mu\text{-NEt}_2)]_2$  (2).** A Schlenk flask was charged with  $[\textit{t}\text{-Bu}(\text{H})\text{Ga}(\mu\text{-NEt}_2)]_2$  (0.43 g, 1.2 mmol) dissolved in 50 mL of  $\text{CHCl}_3$ . The solution was refluxed for 12 h, after which the solvent was removed under vacuum. The crude yellow solid was redissolved in  $\text{CHCl}_3$ , concentrated, and placed in a  $-20^\circ\text{C}$  freezer, where colorless needles of **2** grew. Yield: 97%. Mp:  $202^\circ\text{C}$ .  $^1\text{H}$  NMR ( $\text{C}_6\text{D}_6$ ):  $\delta$  0.93 (t, 6H,  $\text{NCH}_2\text{CH}_3$ , 6.9 Hz), 1.22 (s, 9H,  $\text{C}(\text{CH}_3)_3$ ), 2.82 (dq, 2H,  $\text{NCH}_2\text{CH}_3$ ,  $^2J_{\text{HH}} = 12.9$  Hz,  $^3J_{\text{HH}} = 6.7$  Hz), 3.43 (dq, 2H,  $\text{NCH}_2\text{CH}_3$ ,  $^2J_{\text{HH}} = 12.9$  Hz,  $^3J_{\text{HH}} = 7.0$  Hz).  $^{13}\text{C}$  NMR ( $\text{CDCl}_3$ ):  $\delta$  13.12 ( $\text{NCH}_2\text{CH}_3$ ), 30.19 ( $\text{C}(\text{CH}_3)_3$ ), 42.22 ( $\text{NCH}_2\text{CH}_3$ ). EI MS ( $m/z$ ,  $\text{M}^+ = [\textit{t}\text{-Bu}(\text{Cl})\text{Ga}(\text{NEt}_2)]_2$ ): 433 ( $\text{M}^+ - \text{Cl}$ ), 411 ( $\text{M}^+ - \textit{t}\text{-Bu}$ ), 396 ( $\text{M}^+ - \text{NEt}_2$ ), 340 ( $\text{M}^+ - 2\text{Cl} - \textit{t}\text{-Bu}$ ), 248 ( $\text{ClGa}_2\text{NEt}_2^+$ ), 234 ( $\textit{t}\text{-Bu}(\text{Cl})\text{GaNEt}_2^+$ ), 219 ( $\text{ClGa}_2\text{-NEt}^+$ ), 213 ( $\text{Ga}(\text{NEt}_2)_2^+$ ), 198 ( $\textit{t}\text{-BuGaNEt}_2^+$ ), 177 ( $\text{ClGaNEt}_2^+$ ), 142 ( $\text{GaNEt}_2^+$ ), 126 ( $\textit{t}\text{-BuGa}^+$ ). IR spectrum ( $\text{cm}^{-1}$ , KBr pellet): 2973, 2847, 2710, 1450, 1394, 1384, 1362, 1309, 1293, 1262, 1174, 1108, 1043, 1013, 939, 900, 850, 794, 594, 559. Elemental analysis found (calcd based on  $\text{C}_{16}\text{H}_{38}\text{Cl}_2\text{Ga}_2\text{N}_2$ ): C 37.31 (40.99), N 5.29 (5.98), H 7.55 (8.17), Cl 17.71 (15.12).

**Synthesis of  $\textit{t}\text{-Bu}(\text{Cl})\text{Ga}(\mu\text{-NEt}_2)_2\text{GaCl}_2$  (3).** A Schlenk flask was charged with  $[\text{Cl}_2\text{Ga}(\mu\text{-NEt}_2)]_2$  (1.4 g, 3.2 mmol) dissolved in 50 mL of pentane, and 1.7 M *t*-BuLi in pentane (1.2 mL, 2.6 mmol) was slowly added over a 30-min period. The solution was warmed to room temperature, stirred overnight, and then filtered, and the solvent was removed under vacuum. The crude pale yellow solid was redissolved in pentane, concentrated, and placed in a  $-20^\circ\text{C}$  freezer, where colorless needles of **3** grew. Yield: 47%. Mp: 131

$^1\text{H}$  NMR ( $\text{C}_6\text{D}_6$ ):  $\delta$  0.81 (t, 3 H,  $\text{NCH}_2\text{CH}_3$ , 6.9 Hz), 0.84 (t, 3 H,  $\text{NCH}_2\text{CH}_3$ , 6.9 Hz), 1.09 (s, 9 H,  $\text{C}(\text{CH}_3)_3$ ), 2.75 (dq broad, 1 H,  $\text{NCH}_2\text{CH}_3$ ,  $^2J_{\text{HH}} = 13.2$  Hz,  $^3J_{\text{HH}} = 6.9$  Hz), 2.89 (dq, 1 H,  $\text{NCH}_2\text{CH}_3$ ,  $^2J_{\text{HH}} = 13.8$  Hz,  $^3J_{\text{HH}} = 6.7$  Hz), 3.06 (dq, 1 H,  $\text{NCH}_2\text{CH}_3$ ,  $^2J_{\text{HH}} = 13.2$  Hz,  $^3J_{\text{HH}} = 7.0$  Hz), 3.38 (dq, 1 H,  $\text{NCH}_2\text{CH}_3$ ,  $^2J_{\text{HH}} = 13.8$  Hz,  $^3J_{\text{HH}} = 7.2$  Hz).  $^{13}\text{C}$  NMR ( $\text{C}_6\text{D}_6$ ):  $\delta$  12.46 ( $\text{NCH}_2\text{CH}_3$ ), 12.92 ( $\text{NCH}_2\text{CH}_3$ ), 30.24 ( $\text{C}(\text{CH}_3)_3$ ), 42.42 ( $\text{NCH}_2\text{CH}_3$ ), 43.34 ( $\text{NCH}_2\text{CH}_3$ ). EI MS ( $m/z$ ,  $\text{M}^+ = t\text{-Bu}(\text{Cl})\text{Ga}(\text{NEt}_2)_2\text{-GaCl}_2$ ): 411 ( $\text{M}^+ - \text{Cl}$ ), 389 ( $\text{M}^+ - t\text{-Bu}$ ), 249 ( $\text{ClGa}_2\text{NEt}_2^+$ ), 233 ( $t\text{-Bu}(\text{Cl})\text{GaNEt}_2^+$ ), 213 ( $\text{Ga}(\text{NEt}_2)_2^+$ ), 198 ( $t\text{-BuGaNEt}_2^+$ ), 176 ( $\text{ClGaNEt}_2^+$ ), 140 ( $\text{GaCl}_2^+$ ), 126 ( $t\text{-BuGa}^+$ ), 106 ( $\text{GaCl}^+$ ). IR spectrum ( $\text{cm}^{-1}$ , KBr pellet): 3193, 2977, 2850, 2475, 1594, 1458, 1397, 1363, 1261, 1196, 1061, 979, 796, 680, 614, 516. Elemental analysis found (calcd based on  $\text{C}_{12}\text{H}_{29}\text{Cl}_3\text{Ga}_2\text{N}_2$ ): C 32.57 (31.18), N 5.87 (6.26), H 6.99 (6.53), Cl 21.21 (23.78).

**Alternate Synthesis of 1.** A Schlenk flask was charged with  $[t\text{-Bu}(\text{Cl})\text{Ga}(\mu\text{-NEt}_2)]_2$  (0.184 g, 0.299 mmol) dissolved in 50 mL of pentane at room temperature. To this solution was added 1.7 M  $t\text{-BuLi}$  in pentane (0.35 mL, 0.60 mmol) slowly over a 30-min period. The solution was stirred at room temperature overnight and then filtered, and the solvent was removed under vacuum. The crude pale yellow solid was redissolved in pentane, concentrated, and placed in a  $-20^\circ\text{C}$  freezer, where colorless plates of **1** grew.

**Alternate Synthesis of 2.** A Schlenk flask was charged with  $t\text{-Bu}(\text{Cl})\text{Ga}(\mu\text{-NEt}_2)_2\text{GaCl}_2$  (0.23 g, 0.51 mmol) dissolved in 50 mL of pentane, and 1.7 M  $t\text{-BuLi}$  in pentane (0.35 mL, 0.60 mmol) was slowly added over a 30-min period. The solution was stirred at room temperature overnight and then filtered, and the solvent was removed under vacuum. The crude pale yellow solid was redissolved in pentane, concentrated, and placed in a  $-20^\circ\text{C}$  freezer, where colorless needles of **2** grew.

**X-ray Diffraction Collection and Refinement.** Crystals of **1**, **2**, and **3** suitable for single-crystal X-ray diffraction were obtained by slow cooling from solution (see above). Colorless crystals were mounted on glass capillaries and cooled under a  $\text{N}_2$  cold gas stream during data collection. Data for **1** and **3** were collected on an Enraf-Nonius CAD4 diffractometer using  $\theta$ - $2\theta$  scans. Intensity scans were taken at 2 h intervals, and Lorentz and polarization corrections were applied. Absorption corrections were made using  $\psi$  scans. The MoLEN software package was utilized for data reduction. Data on crystals of **2** were collected using a Nonius KappaCCD diffractometer. Lorentz and polarization corrections were applied to the data. The HKLint software package was used for data reduction.

In each case above, structure solutions were obtained using modules from SHELXTL v5.1. A direct methods program (XS) generated a preliminary model that was refined by least-squares methods (XL). All non-hydrogen atoms were refined with anisotropic thermal parameters. For crystal **1**, the positions of all hydrogens except H1 (attached to Ga1) were included with a riding model using default values and the coordinates of H1 were allowed to vary with the constraint that its isotropic thermal parameter tracked with Ga1 such that  $U_{\text{iso}}(\text{H1}) = 1.2U_{\text{iso}}(\text{Ga1})$ . In the structural representations, the thermal ellipsoids are drawn at 35% levels unless otherwise indicated.

**Thermal Stability and Decomposition Studies.** Thermogravimetric-differential thermal analysis was performed on a Seiko ExStar 6300 system with a  $10^\circ\text{C}/\text{min}$  ramp under flowing argon using milligram amounts of  $[t\text{-Bu}(\text{H})\text{Ga}(\mu\text{-NEt}_2)]_2$ . Chemical vapor deposition studies were carried out in an atmospheric pressure, hot-wall, horizontal flow CVD system, similar to one described previously.<sup>23</sup> The solid precursor was heated to  $130$ – $140^\circ\text{C}$ , and volatile material was transported by the argon carrier gas ( $100$ –

$200$  sccm) to Si(111) and  $\text{SiO}_2$  substrates that were in the center of a heated tube furnace ( $240$ – $250^\circ\text{C}$ ). Volatile byproducts were collected in a cooled ( $-78^\circ\text{C}$ ) trap for offline analysis.

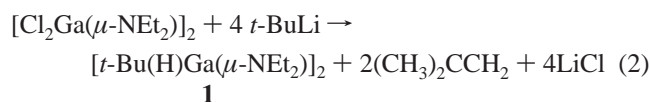
## Results and Discussion

The original target of this study was a sterically bulky diethylamido gallium precursor containing potentially cleavable *tert*-butyl groups ( $-\text{C}(\text{CH}_3)_3$ , *t*-Bu) for use in low-temperature CVD and solution growth of GaN. Initial reactions between  $[t\text{-Bu}_2\text{Ga}(\mu\text{-Cl})]_2$  and  $\text{LiNEt}_2$  were unsuccessful in producing  $[t\text{-Bu}_2\text{Ga}(\mu\text{-NEt}_2)]_2$  and led to intractable oils containing multiple amide species. An alternate approach was examined that involved the construction of an amide-bridged dimer,  $[\text{Cl}_2\text{Ga}(\mu\text{-NEt}_2)]_2$ ,<sup>20</sup> prior to alkylation (eq 1).



Four equivalents of  $t\text{-BuLi}$  was then added to a  $[\text{Cl}_2\text{Ga}(\mu\text{-NEt}_2)]_2$  solution in an attempt to isolate dimeric  $[t\text{-Bu}_2\text{Ga}(\mu\text{-NEt}_2)]_2$ ; however, the only molecular species isolated from this reaction contained *one* *t*-Bu per gallium center and no chlorine. The mass spectrum and elemental analysis of the isolated product indicate one *t*-Bu and one H per gallium, consistent with the formation of a dimeric gallium hydride,  $[t\text{-Bu}(\text{H})\text{Ga}(\mu\text{-NEt}_2)]_2$ , **1**. The  $^1\text{H}$  NMR spectrum of **1** has a broad resonance at 4.73 ppm, which is in the range of Ga–H resonances described in other gallium hydride systems (ca. 4.4–5.4 ppm).<sup>14,16,24</sup> The methylene region is a complex multiplet that simple modeling demonstrated to consist of two partially overlapping doublets of quartets (Figure S1), consistent with an *anti*-hydride configuration.

NMR scale reactions between  $[\text{Cl}_2\text{Ga}(\mu\text{-NEt}_2)]_2$  and  $t\text{-BuLi}$  at room temperature reveal that Ga–H formation is accompanied by isobutylene  $[(\text{CH}_3)_2\text{CCH}_2]$  evolution (1.60 and 4.76 ppm). This suggests that a *tert*-butyl group is sacrificed during hydride formation, perhaps via a  $\beta$ -hydride elimination process (eq 2). There is literature precedence for gallium



hydrides such as  $(2,4,6\text{-}t\text{-Bu}_3\text{C}_6\text{H}_2)_2\text{GaH}$  resulting from  $t\text{-BuLi}$  reaction with a sterically bulky alkyl gallium chloride.<sup>25</sup> A variety of monomeric gallium dihydrides with bulky ligand systems have also been reported, using  $\text{LiGaH}_4$  as the hydride source.<sup>17</sup> The reaction in eq 2 represents a rare example of a hydride-forming reaction using  $t\text{-BuLi}$ .

**Solid-State Structure of  $[t\text{-Bu}(\text{H})\text{Ga}(\mu\text{-NEt}_2)]_2$  (**1**).** Single-crystal X-ray diffraction results show that the solid-state structure of **1** is consistent with solution results, confirming a dimeric, *anti*-hydride, amido-bridged structure with an inversion center (Figure 1). Table 1 lists crystallographic parameters and refinement results, and Table 2 presents selected structural data for **1**. The planar  $\text{Ga}_2\text{N}_2$  core is only

(23) Gillan, E. G.; Barron, A. R. *Chem. Mater.* **1997**, *9*, 3037.

(24) Janik, J. F.; Wells R. L. *Inorg. Chem.* **1997**, *36*, 4135.

(25) Wehmschulte, R. J.; Ellison, J. J.; Ruhlandt-Senge, K.; Power, P. P. *Inorg. Chem.* **1994**, *33*, 6300.

**Table 1.** Crystallographic Data for Dimeric Gallium Amides, **1–3**

parameter	[ <i>t</i> -Bu(H)Ga( $\mu$ -NEt <sub>2</sub> ) <sub>2</sub> ] ( <b>1</b> )	[ <i>t</i> -Bu(Cl)Ga( $\mu$ -NEt <sub>2</sub> ) <sub>2</sub> ] ( <b>2</b> )	[ <i>t</i> -Bu(Cl)Ga( $\mu$ -NEt <sub>2</sub> ) <sub>2</sub> GaCl <sub>2</sub> ] ( <b>3</b> )
chemical formula	C <sub>16</sub> H <sub>40</sub> Ga <sub>2</sub> N <sub>2</sub>	C <sub>16</sub> H <sub>38</sub> Cl <sub>2</sub> Ga <sub>2</sub> N <sub>2</sub>	C <sub>12</sub> H <sub>29</sub> Cl <sub>3</sub> Ga <sub>2</sub> N <sub>2</sub>
fw, g mol <sup>-1</sup>	399.94	468.82	447.16
space group	<i>P</i> 2 <sub>1</sub> / <i>c</i>	<i>P</i> $\bar{1}$	<i>P</i> 2 <sub>1</sub> / <i>c</i>
<i>a</i> , Å	9.327(2)	7.6330(2)	9.625(2)
<i>b</i> , Å	11.661(2)	8.9281(2)	12.122(3)
<i>c</i> , Å	10.229(2)	9.0960(2)	16.540(4)
$\alpha$ , deg	90	85.4870(10)	90
$\beta$ , deg	109.77(2)	73.7860(10)	94.83(2)
$\gamma$ , deg	90	69.1810(10)	90
<i>V</i> , Å <sup>3</sup>	1047.0(4)	556.21(2)	1922.9(8)
<i>Z</i>	2	1	4
<i>D</i> <sub>calcd</sub> , g cm <sup>-3</sup>	1.269	1.400	1.545
$\mu$ , cm <sup>-1</sup>	25.69	26.61	32.10
<i>T</i> , °C	-63	-83	-63
$\lambda$ , Å	0.71073	0.71073	0.71073
<i>R</i> , <i>R</i> <sub>w</sub> [ <i>I</i> > 2 $\sigma$ ( <i>I</i> )] <sup>a</sup>	0.0382, 0.0972	0.0226, 0.0493	0.0325, 0.0871

<sup>a</sup>  $R = \sum ||F_o| - |F_c|| / \sum |F_o|$ ;  $R_w = [\sum w(F_o^2 - F_c^2)^2 / \sum w(F_o^2)]^{0.5}$ ,  $w = [\sigma^2(F_o^2) + (aP)^2 + (bP)]^{-1}$  where  $P = (F_o^2 + 2F_c^2)/3$ . The weighting coefficients (*a*, *b*) for each structure are as follows: **1** (0.0522, 0.92), **2** (0.0082, 0.24), and **3** (0.0480, 1.40).

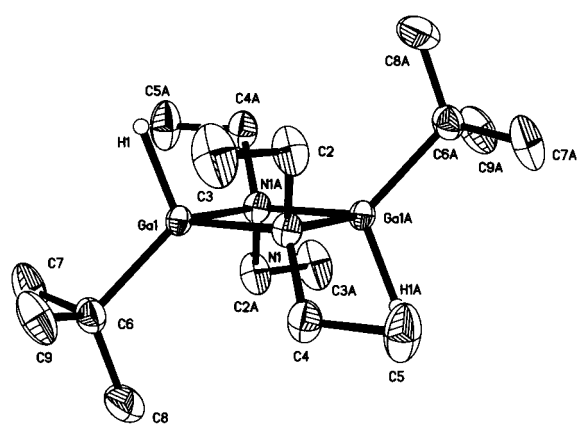


**Figure 1.** View of [*t*-Bu(H)Ga( $\mu$ -NEt<sub>2</sub>)<sub>2</sub>] (**1**) showing the atom-labeling scheme. The hydrogen atoms, except those attached to gallium, are omitted for clarity.

**Table 2.** Selected Bond Lengths and Angles for [*t*-Bu(H)Ga( $\mu$ -NEt<sub>2</sub>)<sub>2</sub>] (**1**)

component	distance (Å) or angle (deg)
Ga(1)–N(1)	2.025(3)
Ga(1)–C(6)	2.001(4)
Ga(1)–H(1)	1.57(4)
Ga(1)–Ga(1a)	2.8851(11)
N(1)–Ga(1)–N(1a)	88.81(13)
Ga(1)–N(1)–Ga(1a)	91.19(13)
C(6)–Ga(1)–H(1)	115.5(15)
N(1)–Ga(1)–H(1)	105.4(15)
N(1)–Ga(1)–C(6)	119.5(2)
C(2)–N(1)–Ga(1)	110.0(3)
C(4)–N(1)–Ga(1)	116.2(3)

slightly distorted from 90° angles, and the Ga–N bond length (2.03 Å) is consistent with those observed in other dimeric dialkylamido-<sup>20,26</sup> and monoalkylamido- or hydrazine-bridged systems.<sup>27</sup> The Ga–H distance in **1** is 1.57 Å, which is at the high end of previously reported terminal Ga–H bonds (ca. 1.4–1.6 Å).<sup>14,18,28,29</sup> For comparison, argon matrix

isolated H<sub>2</sub>GaNH<sub>2</sub> has a calculated 1.56 Å Ga–H bond length based on the observed IR spectrum<sup>30</sup> and 1.57 Å Ga–H bond lengths were predicted for cyclotrigallazane ([H<sub>2</sub>GaNH<sub>2</sub>]<sub>3</sub>).<sup>29</sup>

A variety of crystallographically characterized gallium hydrides with reported IR absorptions are listed in Table 3. These include terminal monohydrides, terminal dihydrides, and various bridging hydride structures. As expected, bridging Ga–H–Ga bonds are considerably longer (ca. 1.6–1.8 Å) than terminal ones. A plot of gallium terminal monohydrides and bridging hydride bond lengths versus IR absorption energies is shown in Figure 2. There is considerable scatter in part due to the difficulty in accurately determining Ga–H bond lengths; however, the general trend is that increasing Ga–H bond lengths track with decreasing vibrational energies. The Ga–H IR stretch for **1** occurs at 1834 cm<sup>-1</sup>, which is lower than observed for other terminal gallium hydrides (ca. 1850–1900 cm<sup>-1</sup>, Table 3). The *tert*-butyl groups and Lewis basicity of its alkylamido bridges may enhance electron density at gallium and promote weaker, more covalent metal–hydrogen interactions. For reference, the Ga–H distance in **1** (1.57 Å) is nearly equal to the sum of their covalent radii (1.55–1.57 Å).<sup>31</sup>

**Atmospheric Stability of [*t*-Bu(H)Ga( $\mu$ -NEt<sub>2</sub>)<sub>2</sub>].** Gallium amides are often quite sensitive toward hydrolysis, leading to the formation of free amine and gallium hydroxides. Gallium hydrides also have a tendency to oligomerize or decompose; for example, gallium coordinated to a phosphorus–nitrogen macrocycle decomposes to gallium metal soon after Ga–H formation,<sup>32</sup> and cyclotrigallazane produces polymeric material with H<sub>2</sub> and NH<sub>3</sub> loss.<sup>11a</sup> There is a report,

- (26) (a) Waggoner, K. M.; Olmstead, M. M.; Power, P. P. *Polyhedron* **1990**, *9*, 257. (b) Nutt, W. R.; Murry, K. J.; Gulick, J. M.; Odom, J. D.; Ding, Y.; Lebioda, L. *Organometallics* **1996**, *15*, 1728.  
 (27) (a) Atwood, D. A.; Jones, R. A.; Cowley, A. H.; Bott, S. G.; Atwood, J. L. *Polyhedron* **1991**, *10*, 1897. (b) Atwood, D. A.; Atwood, V. O.; Cowley, A. H.; Jones, R. A.; Atwood, J. L.; Bott, S. G. *Inorg. Chem.* **1994**, *33*, 3251. (c) Peters, D. W.; Bourret, E. D.; Power, M. P.; Arnold, J. J. *Organomet. Chem.* **1999**, *582*, 108.

- (28) Baxter, P. L.; Downs, A. J.; Rankin, D. W. H.; Robertson, H. E. *J. Chem. Soc., Dalton Trans.* **1985**, 807.  
 (29) (a) Hwang, J.-W.; Hanson, S. A.; Britton, D.; Evans, J. F.; Jensen, K. F.; Gladfelter, W. L. *Chem. Mater.* **1990**, *2*, 342. (b) Campbell, J. P.; Hwang, J.-W.; Young, V. G., Jr.; Von Dreele, R. B.; Cramer, C. J.; Gladfelter, W. L. *J. Am. Chem. Soc.* **1998**, *120*, 521.  
 (30) Himmel, H.-J.; Downs, A. J.; Greene, T. M. *Chem. Commun.* **2000**, 871.  
 (31) (a) Emsley, J. *The Elements*; Clarendon Press: New York, 1989. (b) *Handbook of Chemistry and Physics*, 66th ed.; Weast, R. C., Ed.; CRC Press: Boca Raton, FL, 1985.  
 (32) Fryzuk, M. D.; Giesbrecht, G. R.; Rettig, S. J.; Yap, G. P. A. *J. Organomet. Chem.* **1999**, *591*, 63.

**Table 3.** Comparison of Structurally Characterized Gallium–Hydrogen Bond Lengths and IR Stretching Frequencies

compound	Ga–H bond length (Å)	Ga–H IR (cm <sup>-1</sup> )	ref
Terminal Ga–H Monomers			
[2,6-(Me <sub>2</sub> NCH <sub>2</sub> ) <sub>2</sub> C <sub>6</sub> H <sub>3</sub> ]GaH <sub>2</sub>	1.418(39)	1837, 1854	17a
Ga(H)(S- <i>t</i> -Bu) <sub>2</sub> (NMe <sub>3</sub> )	1.48(3)	1884	18
H <sub>x</sub> Ga[N(SiMe <sub>3</sub> ) <sub>2</sub> ] <sub>3-x</sub> (quin)	<i>x</i> = 1: 1.49(2)	1893	14b
(quin = quinuclidine)	<i>x</i> = 2: 1.473(2), 1.46(2)	1855, 1872	
(2,4,6- <i>t</i> -Bu <sub>3</sub> C <sub>6</sub> H <sub>3</sub> ) <sub>2</sub> GaH	1.572(48)	1867	25
Terminal Ga–H Dimers			
[H <sub>2</sub> Ga(H)NMe <sub>2</sub> ] <sub>2</sub>	1.51(3)	1897, 1912	14a
{[(Me <sub>3</sub> Si) <sub>2</sub> N](H)Ga[N(H)CH <sub>2</sub> CH <sub>2</sub> CH <sub>2</sub> NMe <sub>2</sub> ]} <sub>2</sub>	1.51(3)	1903	16
[ <i>t</i> -Bu(H)Ga(μ-NEt <sub>2</sub> ) <sub>2</sub> ] <sub>2</sub>	1.57(4)	1834	this work
Terminal Ga–H Trimers and Tetramers			
[H <sub>2</sub> Ga(μ-NH <sub>2</sub> ) <sub>3</sub> ] <sub>3</sub>	1.40(6)	1865, 1889	29b
[ <i>t</i> -Bu <sub>2</sub> Ga(μ-H)] <sub>2</sub> [Ga(μ-H)( <i>H</i> )- <i>t</i> -Bu] <sub>2</sub>	1.44(10), 1.73(11)	1907	19
Bridging Ga–H–Ga Structures			
[(2,4,6- <i>i</i> -Pr <sub>3</sub> C <sub>6</sub> H <sub>3</sub> ) <sub>2</sub> Ga(μ-H)] <sub>2</sub>	1.650(70)–1.792(70)	1755	25
[ <i>t</i> -Bu <sub>2</sub> Ga(μ-H)] <sub>2</sub> [Ga(μ-H)( <i>H</i> )- <i>t</i> -Bu] <sub>2</sub>	1.69(5)–1.82(4)	1649	19

however, of sterically bulky monomeric gallium hydride that exhibits good photolytic and thermal stability.<sup>17a</sup>

In contrast to many metal hydrides, the Ga–H bond in **1** is significantly air-stable under ambient conditions. Solid samples of **1** that were exposed to laboratory atmosphere for three weeks still showed predominantly [*t*-Bu(H)Ga(μ-NEt<sub>2</sub>)<sub>2</sub>]<sub>2</sub>, including the Ga–H <sup>1</sup>H NMR resonance, with only slight evidence of decomposition. In addition, bubbling dry O<sub>2</sub> through a C<sub>6</sub>D<sub>6</sub> solution of **1** produced no observable decomposition or change in the <sup>1</sup>H NMR. Bubbling gaseous NH<sub>3</sub> through a pentane solution of **1** at room temperature produced a small amount of white precipitate that retained Ga–H and Ga–NEt<sub>2</sub> IR signatures and showed no evidence of N–H formation. One new peak in the IR appeared at 2080 cm<sup>-1</sup>; however, the mass spectra and <sup>1</sup>H NMR of this insoluble material only showed evidence of **1**. The soluble (major) portion consisted of **1** with minor evidence of a new diethylamido species. Solution photolysis and sonication also had no detectable effect on **1**. The chemical stability of **1** may be a consequence of protection by sterically bulky hydrophobic *tert*-butyl and diethylamido ligands that partially shield the Ga–H bond from hydrolysis and oxidation. As Figure 1 shows, each ethyl group of [*t*-Bu(H)Ga(μ-NEt<sub>2</sub>)<sub>2</sub>]<sub>2</sub> is bent toward the less sterically hindered Ga–H bond.

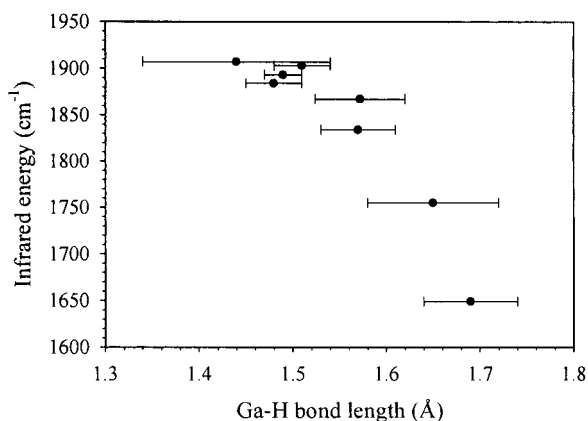
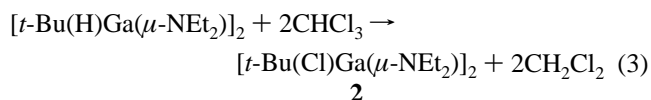


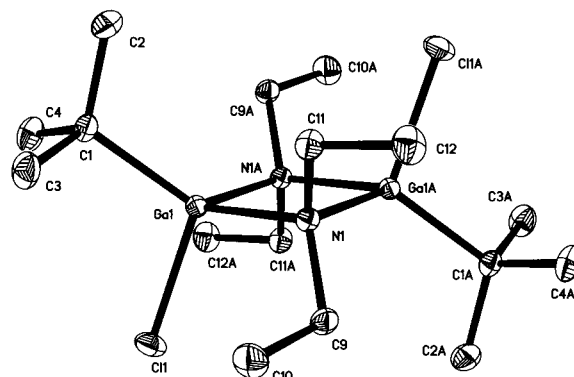
**Figure 2.** Comparison of the IR absorption near 1800 cm<sup>-1</sup> versus crystallographic Ga–H bond lengths for a series of terminal monohydrides and bridging hydrides. When multiple IR energies or bond lengths are listed in Table 3, the smallest bond length and largest IR energy are plotted.

**Solution Reactivity of [*t*-Bu(H)Ga(μ-NEt<sub>2</sub>)<sub>2</sub>]<sub>2</sub>.** The presence and reactivity of the Ga–H bond in **1** was probed by monitoring its reaction with chloroform. After room temperature dissolution of **1** in CDCl<sub>3</sub>, the <sup>1</sup>H NMR spectra exhibited new peaks for CDHCl<sub>2</sub> and a corresponding loss of the Ga–H resonance. The large-scale reaction of **1** with CHCl<sub>3</sub> resulted in a dichloro amido-bridged dimer (eq 3).



The <sup>1</sup>H NMR and EI-MS of **2** are consistent with the formation of [*t*-Bu(Cl)Ga(μ-NEt<sub>2</sub>)<sub>2</sub>]<sub>2</sub> with *trans tert*-butyl groups. As with **1**, the methylene multiplets were modeled as doublets of quartets, consistent with an *anti*-chloride structure (Figure S2). The solid-state structure of **2** verified that the *anti* geometry is present in the solid state (Figure 3). Selected crystallographic data and structural features are presented in Tables 1 and 4. Note that the Ga–H bond could not be re-formed from **2** by direct reaction with CaH or NaAlH<sub>4</sub>.

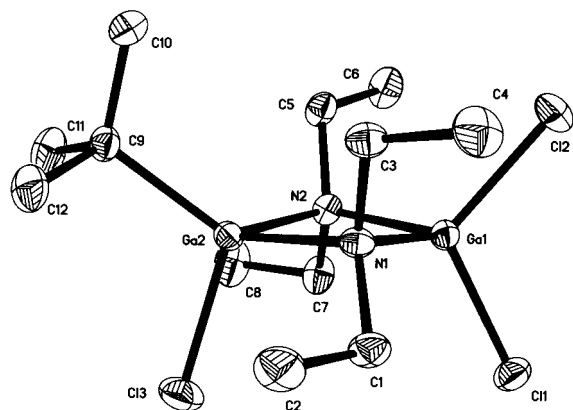
***t*-BuLi Additions to [Cl<sub>2</sub>Ga(μ-NEt<sub>2</sub>)<sub>2</sub>]<sub>2</sub>.** Several attempts were made to directly generate partially substituted *tert*-butyl gallium amides. The direct reaction of [Cl<sub>2</sub>Ga(μ-NEt<sub>2</sub>)<sub>2</sub>]<sub>2</sub> with 1 equiv of *t*-BuLi resulted in a monosubstituted dimer (eq



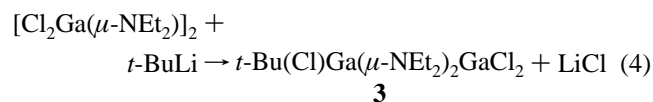
**Figure 3.** View of [*t*-Bu(Cl)Ga(μ-NEt<sub>2</sub>)<sub>2</sub>]<sub>2</sub> (**2**) showing the atom-labeling scheme. The hydrogen atoms are omitted for clarity.

**Table 4.** Selected Bond Lengths (Å) and Angles (deg) for  $[t\text{-Bu}(\text{Cl})\text{Ga}(\mu\text{-NEt}_2)_2]_2$  (**2**) and  $t\text{-Bu}(\text{Cl})\text{Ga}(\mu\text{-NEt}_2)_2\text{GaCl}_2$  (**3**)

$[t\text{-Bu}(\text{Cl})\text{Ga}(\mu\text{-NEt}_2)_2]_2$ ( <b>2</b> )		$t\text{-Bu}(\text{Cl})\text{Ga}(\mu\text{-NEt}_2)_2\text{GaCl}_2$ ( <b>3</b> )	
Ga(1)–N(1)	2.0218(11)	Ga(1)–N(1)	1.980(2)
Ga(1)–N(1a)	2.0205(11)	Ga(1)–N(2)	1.971(2)
		Ga(2)–N(1)	2.043(2)
		Ga(2)–N(2)	2.037(2)
Ga(1)–C(1)	1.9983(14)	Ga(2)–C(9)	1.997(2)
Ga(1)–Cl(1)	2.2297(4)	Ga(1)–Cl(1)	2.1527(8)
		Ga(1)–Cl(2)	2.1582(8)
		Ga(2)–Cl(3)	2.2022(8)
Ga(1)–Ga(1a)	2.8880(3)	Ga(1)–Ga(2)	2.8519(7)
N(1)–Ga(1)–N(1a)	88.81(4)	N(1)–Ga(1)–N(2)	90.77(9)
		N(1)–Ga(2)–N(2)	87.15(8)
Ga(1)–N(1)–Ga(1a)	91.19(4)	Ga(1)–N(1)–Ga(2)	90.28(8)
		Ga(1)–N(2)–Ga(2)	90.70(8)
C(1)–Ga(1)–Cl(1)	109.29(4)	C(9)–Ga(2)–Cl(3)	111.25(8)

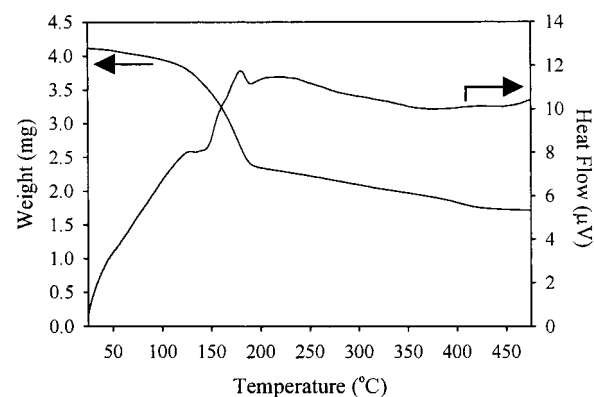
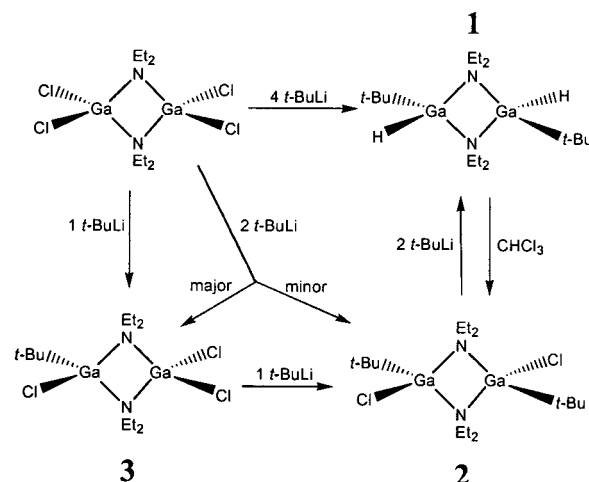
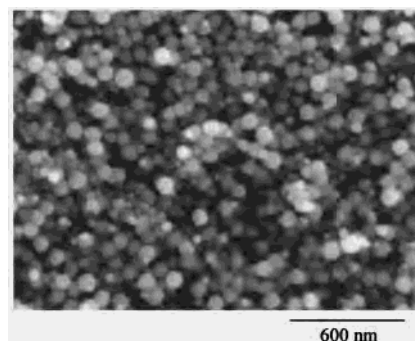
**Figure 4.** View of  $t\text{-Bu}(\text{Cl})\text{Ga}(\mu\text{-NEt}_2)_2\text{GaCl}_2$  (**3**) showing the atom-labeling scheme. The hydrogen atoms are omitted for clarity.

4). The structure of **3** shows features similar to the gallium



dimers discussed above (Figure 4, Tables 1 and 4). Due to the asymmetric substitution, there is some distortion of the  $\text{Ga}_2\text{N}_2$  ring planarity and it is slightly bowed away ( $11.3^\circ$ ) from the lone *tert*-butyl group and all four methylene resonances are separate doublets of quartets (Figure S3). Surprisingly, when 2 equiv of *t*-BuLi is added to  $[\text{Cl}_2\text{Ga}(\mu\text{-NEt}_2)]_2$ , **3** is still the major isolable product and only a minor amount of **2** is observed. However, **2** can be prepared by a subsequent addition of 1 equiv of *t*-BuLi to **3**. When **2** is placed in  $\text{C}_6\text{D}_6$  with 2 equiv of *t*-BuLi, isobutylene and Ga–H resonances appear in the NMR spectrum. On a larger scale, the addition of two *t*-BuLi to  $[t\text{-Bu}(\text{Cl})\text{Ga}(\mu\text{-NEt}_2)]_2$  also yields  $[t\text{-Bu}(\text{H})\text{Ga}(\mu\text{-NEt}_2)]_2$ . A summary of the various conversions is shown in Scheme 1.

**Thermal Stability and Preliminary Decomposition Studies.** Thermogravimetric-differential thermal analysis (TG-DTA) and melting point measurements indicate that  $[t\text{-Bu}(\text{H})\text{Ga}(\mu\text{-NEt}_2)]_2$  melts irreversibly at  $150\text{--}160^\circ\text{C}$  and decomposes above  $200^\circ\text{C}$  (Figure 5). This small window of stability was utilized to perform exploratory chemical vapor deposition (CVD) studies with **1**. This precursor deposits gallium-containing films at low temperatures ( $240\text{--}$

**Scheme 1****Figure 5.** Thermogravimetric-differential thermal analysis of  $[t\text{-Bu}(\text{H})\text{Ga}(\mu\text{-NEt}_2)]_2$  in flowing argon.**Figure 6.** Scanning electron micrograph of a film deposited on silicon from **1** at  $250^\circ\text{C}$ .

$250^\circ\text{C}$ ) that have a smooth morphology with distinct spherical features on the order of  $100\text{ nm}$  (Figure 6). The air-exposed films contain gallium, oxygen, carbon, and a small amount of nitrogen as detected by X-ray photoelectron (XPS) and Auger spectroscopy (Figure S4, Supporting Information). While the  $\text{N}_{1s}$  XPS peak overlaps with the  $\text{Ga}_{\text{LMM}}$  Auger line, there is a small peak at  $1107\text{ eV}$  consistent with  $\text{N}_{\text{KLL}}$  (Auger) emission.<sup>33</sup> A small nitrogen peak is also observed in the Auger survey spectrum. After argon ion sputtering, the XPS surface carbon peak is completely removed and oxygen content is lower (Figure S4). The dark

(33) *Handbook of X-ray Photoelectron Spectroscopy*; Perkin Elmer Corp.—Physical Electronics Division: Eden Prairie, MN, 1992.

yellow films are amorphous by powder X-ray diffraction, and the UV–vis spectra of films on SiO<sub>2</sub> show greater than 50% transmission at 700 nm and a drop below 10% transmission by 380 nm, consistent with GaN ( $E_g = 3.4$  eV, 365 nm) or Ga<sub>2</sub>O<sub>3</sub><sup>34</sup> absorption characteristics. A film grown on Si has a broad IR absorption centered at 600 cm<sup>-1</sup>, which is near the Ga–N and Ga–O stretching regions. NMR analysis of the CVD exhaust products showed evidence for Et<sub>2</sub>NH formation, which suggests a thermal amine elimination process involving the hydride (eq 5). On the basis of



the above data, the films likely consist of partially oxidized gallium spherical nanostructures containing negligible amounts of nitrogen. These results suggest that it will be necessary to add an external nitrogen source, such as NH<sub>3</sub>, in order to obtain stoichiometric GaN films to depositions using **1**.

### Conclusions

Organometallic gallium amides have long been known with a variety of structures and stabilities. In the subset

(34) (a) Valet, M.; Hoffman, D. M. *Chem. Mater.* **2001**, *13*, 2135. (b) Miinea, L.; Suh, S.; Bott, S. G.; Liu, J.-R.; Chu, W.-K.; Hoffman, D. M. *J. Mater. Chem.* **1999**, *9*, 929.

including gallium hydrides, stability and structure are similarly variable. Here we report the formation of a dimeric diethylamido gallium hydride, [t-Bu(H)Ga(μ-NEt<sub>2</sub>)<sub>2</sub>]<sub>2</sub>, that appears to form via β-hydride elimination of a *tert*-butyl group. This structure may be synthesized directly or by the sequential addition of *tert*-butyl substituents to [Cl<sub>2</sub>Ga(μ-NEt<sub>2</sub>)<sub>2</sub>]<sub>2</sub>. Several intermediates are structurally characterized, in addition to the parent hydride. Preliminary chemical vapor deposition studies with [t-Bu(H)Ga(μ-NEt<sub>2</sub>)<sub>2</sub>]<sub>2</sub> resulted in gallium-rich films and demonstrated that Et<sub>2</sub>NH is a facile leaving group.

**Acknowledgment.** The authors thank the Research Corporation (E.G.G., Research Innovation Award), the Office of Naval Research (N00014-99-1-0953), and the University of Iowa for partial support for this work. Dr. Richard Haasch at the Center for Microanalysis of Materials (University of Illinois) is acknowledged for assistance with the XPS measurements.

**Supporting Information Available:** Listings of X-ray crystallographic data (CIF) for the structural determination of **1**, **2**, and **3**, <sup>1</sup>H NMR spectra and NUTS simulation results (data and spectra) for **1**, **2**, and **3**, and surface analysis plots (Auger and XPS) for CVD grown films from **1**. This material is available free of charge via the Internet at <http://pubs.acs.org>.

IC011278A